Cai et al Supporting Information

SUPPLEMENTAL METHODS

Morphometric analysis

Six bright field images of toluidine blue-stained sections were captured from each eye using a Zeiss Axiophot® epifluorescence microscope and a 63x oil immersion objective lens. Images were 100 μm^2 in area and were collected both nasally and temporally at distances of 200, 400, and 600 μm from the optic nerve head. Three measurements of outer nuclear layer (ONL) rows were taken from each image by an observer masked to sample identity (treatment *vs*. control group), then averaged. For each treatment group and age, 2-3 injected eyes were analyzed. Due to variations in injection success and injection site, data from representative individual injected eyes are presented; the average of 3-5 contralateral uninjected eyes (± S.D., *shaded in gray*) is shown for comparison.

Behavioral Testing Methodology

Visual acuities and contrast sensitivities were measured for injected and uninjected mice by observing the optomotor response to a rotating sine-wave grating using the OptoMotry© system (Cerebral Mechanics, Lethbride, Alberta Canada) (1, 2). Mice were placed on a pedestal inside the apparatus and underwent testing by an observer masked to treatment group using a two-alternative forced choice protocol described in detail elsewhere (3-5). Briefly, in this protocol the OptoMotry system presents the mouse with a 5s stimulus rotating in a randomly chosen direction (counter-clockwise or clockwise) at a pre-determined speed, spatial frequency, contrast, and luminance (photopic conditions in these tests). The observer chooses the direction of the stimulus based on observation of the optomotor response of the mouse. The system uses a staircase paradigm to converge on the visual acuity or contrast sensitivity of the mouse (depending on which test is being performed) by automatically adjusting the spatial frequency (acuity) or contrast (contrast sensitivity) after each trial. For acuity testing, the initial spatial frequency is set to 0.200 cycles/degree,while for contrast sensitivity testing the initial contrast is set to 100%. The differential sensitivity of the right and left eye to the rotating grating (left eye more sensitive to clockwise rotation, right eye more sensitive

to counter-clockwise rotation) enables assessment of acuity and contrast sensitivity independently in each eye. Each animal underwent a minimum of eight tests for each protocol. The eight tests were averaged to achieve an acuity/contrast sensitivity value for each mouse.

SUPPLEMENTAL FIGURES AND LEGENDS

Supplemental Figure 1

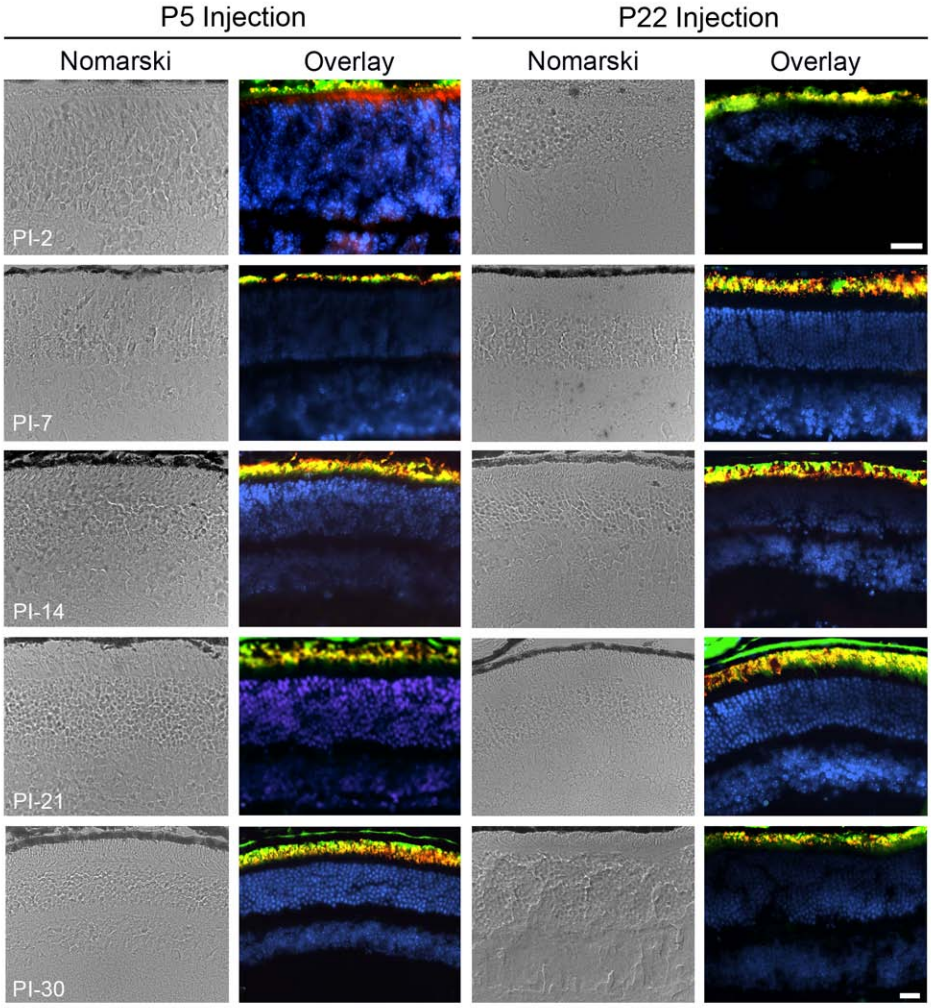

Supplemental Figure 1. Frozen sections were stained with RDS-CT (*red*) and mAB 3B6 (*green*) as described for figure 2. Nomarski images are shown here coupled with the overlay images from nanoparticle injected eyes from figure 2 as a representation of tissue structure. Scale bars, 20 μm.

Supplemental Figure 2

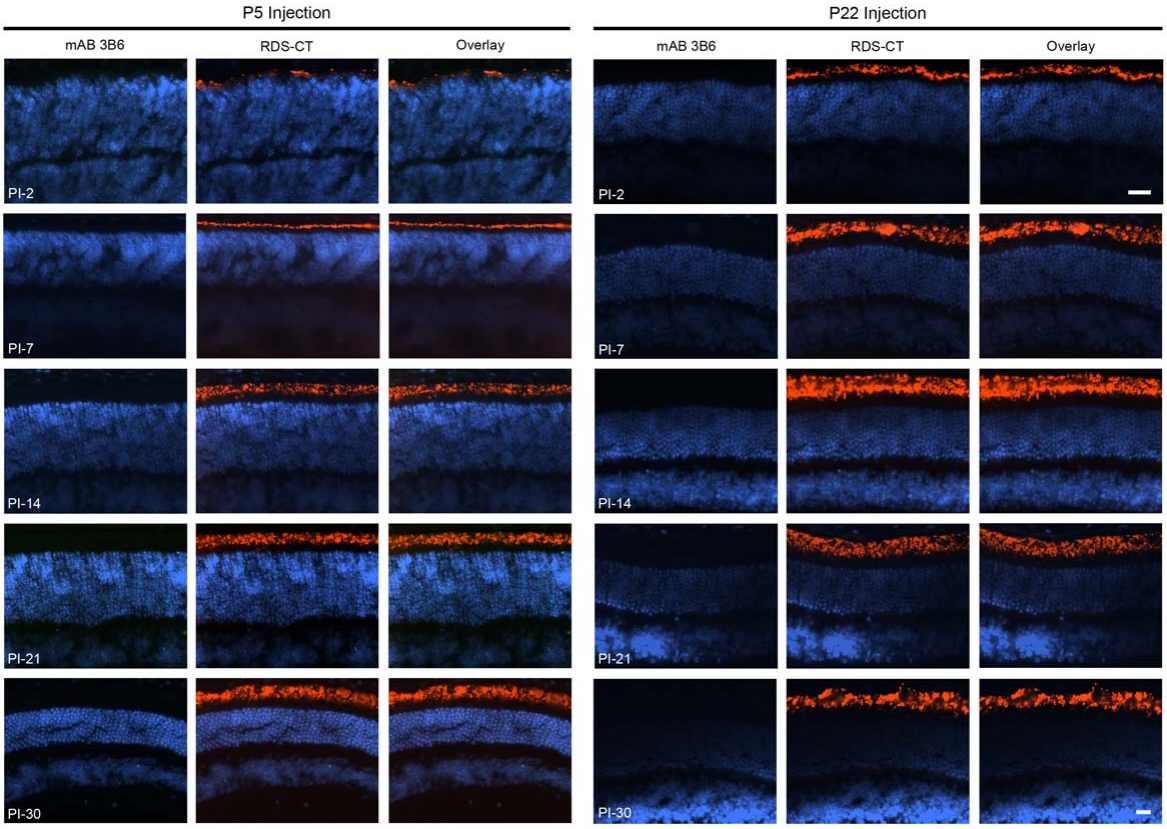

Supplemental Figure 2. Frozen sections were stained with RDS-CT (*red*) and mAB 3B6 (*green*) as described in figure 2. Shown here are images from the individual channels for the naked DNA treated eyes presented in figure 2. Scale bars, 20 μm.

Supplemental Figure 3

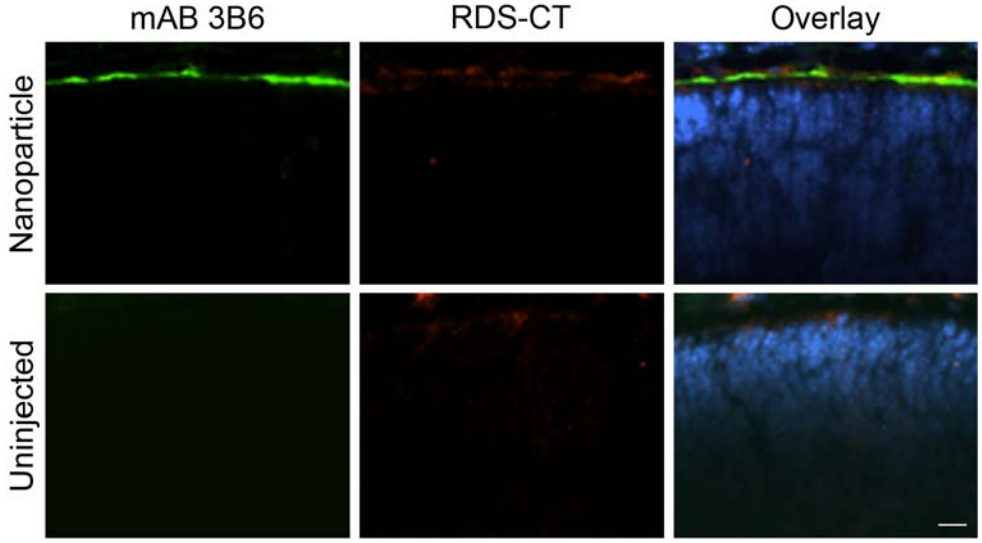

Supplemental Figure 3. *rds*$^{+/-}$ eyes were injected with MOP-NMP nanoparticles at P2. Eyes were collected, cryosectioned and stained with RDS-CT (*red*) and mAB 3B6 (*green*) at PI-2. Transgene is present in nanoparticle injected eyes (*top left panel*) while endogenous RDS is not yet detected (*bottom panels*). Scale bar, 20 μm.

Supplemental Figure 4

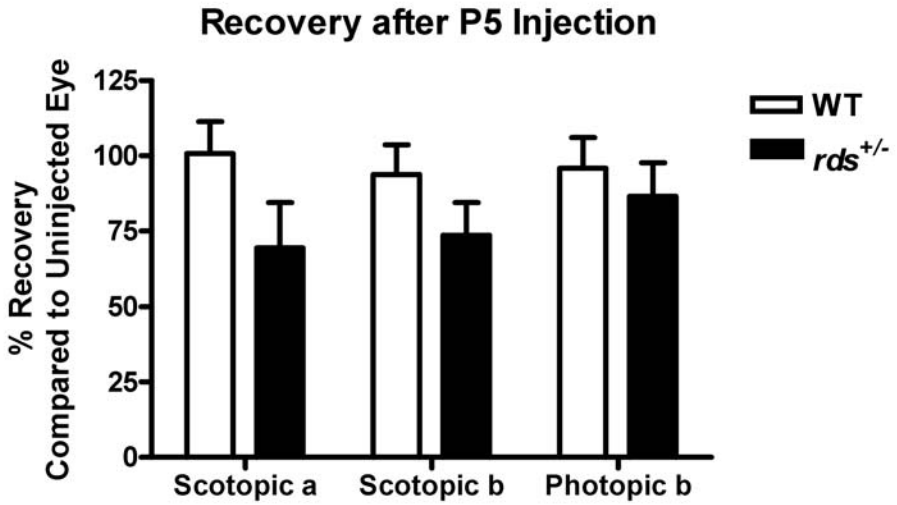

Supplemental Figure 4. One eye of WT and *rds*$^{+/-}$ animals was injected with saline at P5 as described in *Materials & Methods.* At PI-30 animals underwent scotopic and photopic ERG testing. Shown is average percent recovery (compared to the uninjected contralateral eye). While WT eyes fully recover by PI-30, ERG amplitudes in injected *rds*$^{+/-}$ eyes remain lower than in uninjected controls. N=3 mice per group.

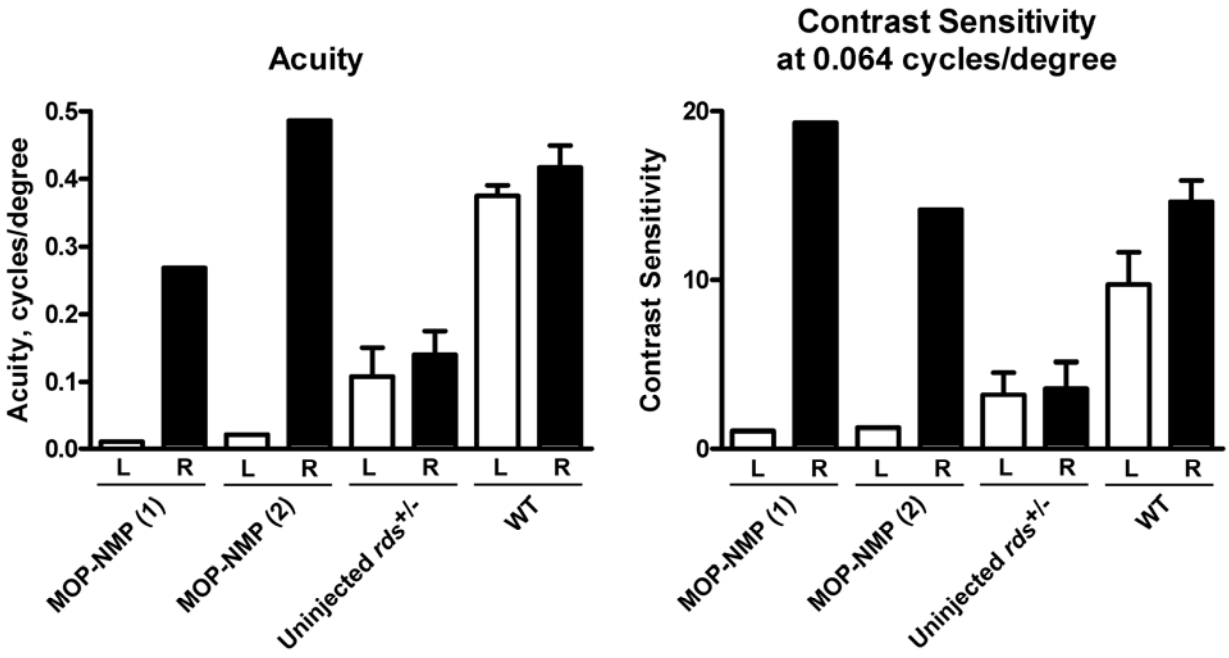

Supplemental Figure 5. Improvement in visual behavior after treatment with MOP-NMP nanoparticles. Two *rds*$^{+/-}$ mice were injected at P5 with MOP-NMP nanoparticles in their right eyes (R), while the left eyes (L) were untreated. These mice, plus five uninjected *rds*$^{+/-}$ mice and four WT untreated mice underwent visual behavior testing under photopic conditions at 9-10 months of age using the optomotor response testing protocol described in the supplemental methods. Uninjected and WT values shown are the average +/- S.E.M. for five and four mice each (respectively) while MOP-NMP (1), and (2) are values for individual injected animals. The two MOP-NMP injected eyes exhibited visual acuities (*left panel*) and contrast sensitivities (*right panel*) substantially higher than the untreated control animals and similar to those observed in the WT animals.

Supplemental Figure 6

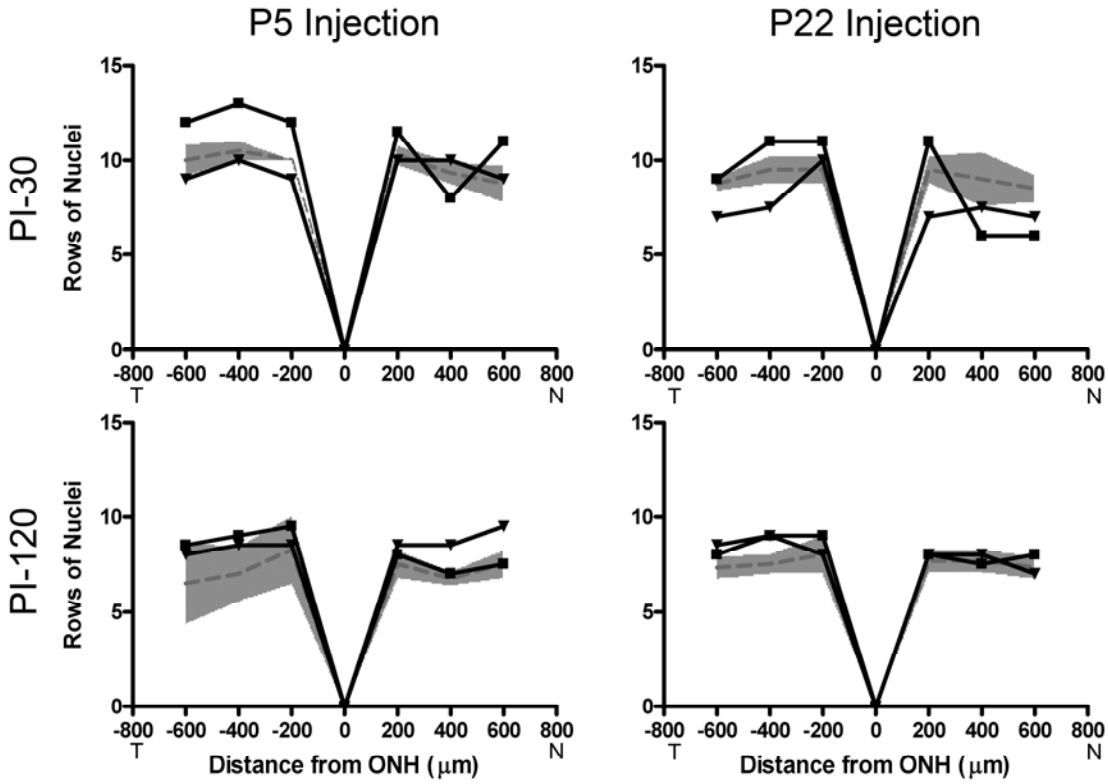

Supplemental Figure 6. Morphometric analysis of nanoparticle-injected eyes. To give an idea of the range seen in normal (untreated) *rds*$^{+/-}$ eyes, the average rows of nuclei from 3-5 uninjected contralateral control eyes is shown by the gray dashed line, ± standard deviation (*shaded in gray*). Black lines represent results from two individual nanoparticle-injected animals, one which demonstrated improvement and one which did not. N, nasal side; T, temporal side. At both PI-30 modest increases in the number of rows of nuclei are detected on the side of injection (T), while at PI-120 improvement is not observed.

Supplemental Figure 7

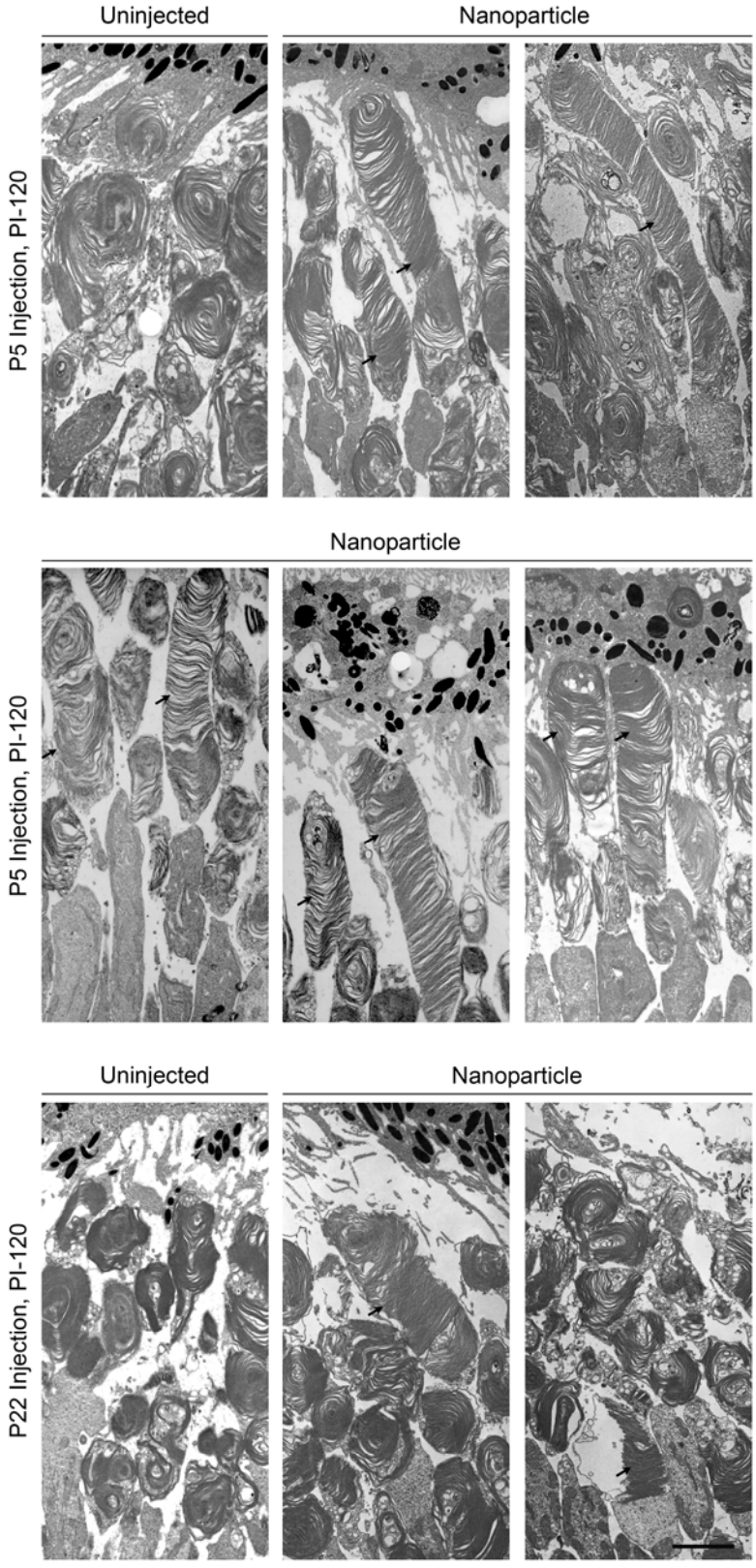

Supplemental Figure 7. Nanoparticle-injected or uninjected eyes were collected and processed for EM as described in figure 7 and *Materials & Methods*. Shown are representative examples of rod OSs from the temporal side of eyes collected at PI-120 after nanoparticle injection at P5 (*top two rows*) or P22 (*bottom row*). Images representing the uninjected eye were obtained from the temporal side of age-matched control animals. Arrows denote improved OS structure. Scale bar, 10μm.

SUPPLEMENTAL REFERENCES

1. Prusky, G. T., Alam, N. M., Beekman, S., and Douglas, R. M. (2004) Rapid quantification of adult and developing mouse spatial vision using a virtual optomotor system. *Investigative ophthalmology & visual science* **45**, 4611-4616
2. Prusky, G. T., and Douglas, R. M. (2004) Characterization of mouse cortical spatial vision. *Vision research* **44**, 3411-3418
3. Alexander, J. J., Umino, Y., Everhart, D., Chang, B., Min, S. H., Li, Q., Timmers, A. M., Hawes, N. L., Pang, J. J., Barlow, R. B., and Hauswirth, W. W. (2007) Restoration of cone vision in a mouse model of achromatopsia. *Nat Med* **13**, 685-687
4. Umino, Y., Frio, B., Abbasi, M., and Barlow, R. (2006) A two-alternative, forced choice method for assessing mouse vision. *Adv Exp Med Biol* **572**, 169-172
5. Umino, Y., Solessio, E., and Barlow, R. B. (2008) Speed, spatial, and temporal tuning of rod and cone vision in mouse. *J Neurosci* **28**, 189-198